SIAM J. MATH. ANAL.
Vol. 56, No. 6, pp. 7290–7305

IDENTIFICATION OF NONLINEAR BEAM-HARDENING EFFECTS IN X-RAY TOMOGRAPHY*

YIRAN WANG†

Abstract. We study streaking artifacts caused by beam-hardening effects in X-ray computed tomography (CT). The effect is known to be nonlinear. We show that the nonlinearity can be recovered from the observed artifacts for strictly convex bodies. The result provides a theoretical support for removal of the artifacts.

Key words. beam-hardening effect, X-ray tomography, nonlinearity, microlocal analysis

MSC codes. 44A12, 46F30

DOI. 10.1137/23M1596491

1. Introduction.

In X-ray computed tomography (CT), artifacts due to beam-hardening effects are common in imaging of patients with medical implants. These artifacts are notorious for causing degradation of CT images and difficulties with diagnosis. The reduction or removal of such artifacts has drawn numerous research efforts, but the problem still remains one of the major challenges in X-ray CT.

In a seminal paper [12], Park, Choi, and Seo demonstrated the nonlinear nature of beam-hardening effects. Let f be the attenuation coefficient of the object being imaged. Because of the polychromatic nature of X-ray beams, we consider the dependency of f on the energy level E. This is particularly significant for metal objects. Assume that $E \in [E_0 - \epsilon, E_0 + \epsilon]$, $\epsilon > 0$, and write f as f_E. Assume that $f_E(x) = f_{E_0}(x) + \alpha(E - E_0)\chi_D$, where χ_D is the characteristic function for a metal object $D \subset \mathbb{R}^2$, and α is a constant which can be thought of as the approximation of the derivative of f_E in E. The X-ray data can be derived from the Beer–Lambert law which gives

$$P = Rf_E + P_{MA}. \tag{1}$$

Here, Rf_E denotes the Radon transform of f_E, and P_{MA} denotes a mismatch term. Under further assumptions, it is derived in [12] that

$$P_{MA} = -\ln\left(\frac{\sinh(\alpha\epsilon R\chi_D)}{\alpha\epsilon R\chi_D}\right) \tag{2}$$

is a nonlinear function of $R\chi_D$. If one applies the filtered back-projection (FBP) to reconstruct f_E, the mismatch term P_{MA} leads to the artifact; see Figure 1 for a demonstration. By using the notion of wave front set in microlocal analysis, the authors of [12] gave a mathematical characterization of the artifacts. For strictly convex objects, the artifacts appear to be straight lines tangent to at least two boundary points of the metal objects; see Figure 1. For more complicated situations, the artifacts and their relation to the geometry of metal regions are further studied in [11, 19]. Finally,

*Received by the editors August 25, 2023; accepted for publication (in revised form) August 2, 2024; published electronically November 1, 2024.
https://doi.org/10.1137/23M1596491
Funding: This work was partially supported by the National Science Foundation (NSF) under grant DMS-2205266.
†Department of Mathematics, Emory University, Atlanta, GA 30322 USA (yiran.wang@emory.edu).

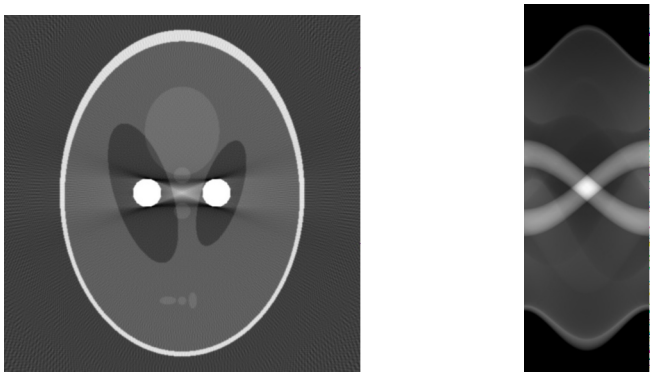

FIG. 1. *Illustration of the beam-hardening artifacts produced by a quadratic nonlinearity. The left figure shows the reconstruction from FBP. The two bright disks represents the metal objects. The artifacts appear to be straight lines tangent to both disks. The right figure shows the sinogram (color map of P in* (1)*). The two bright strips correspond to the support of $R\chi_D$.*

we mention that artifacts due to a similar mechanism are also known in attenuated X-ray tomography; see [7].

The identification of the nonlinear effect in P_{MA} is key to removal of the artifacts. In practice, the shape of the metal objects can usually be acquired, so it is reasonable to assume that χ_D is known and to think of P_{MA} as a nonlinear function $F(R\chi_D)$. Then one can remove P_{MA} if F is known. For example, the numerical scheme developed in [13] consists of two steps: first, one recovers χ_D from the reconstruction f_{CT} using image segmentation techniques; second, one can use the model (2) and find the optimal α which reduces the artifact. The model (2) was derived under certain assumptions. In general, not much can be said about the nonlinear function as it depends on many factors, such as the energy distribution of X-ray beams, geometry, physical properties of metal objects, and even f_{E_0}. Currently, increased effort has been made to find the nonlinear effect by using deep learning techniques; see, for example, [14, 20].

The purpose of this note is to show that the nonlinearity can be identified from the observed artifacts. Also, we provide a constructive proof, which may be potentially seful in practice.

2. The main result. Because of the local nature of the problem as we explain later, it suffices to state our main result in a relatively simple setting. We assume that the metal region $D = D_1 \cup D_2$, where $D_j, j = 1, 2$, are simply connected disjoint bounded domains in $\mathbb{R}^2$ with smooth boundary ∂D_j. Let $\chi_D = \chi_{D_1} + \chi_{D_2}$ be the characteristic function of D. We assume that the attenuation coefficient is of the form

$$f(x) = h(x) + g(x)\chi_D(x), \quad x \in \mathbb{R}^2, \tag{3}$$

where $h, g \in C_0^\infty(\mathbb{R}^2)$. We remark that the form of f is not important for our analysis. We take (3) mainly because it is close to the form in [12]. For the Radon transform on $\mathbb{R}^2$, we use the following parametrization:

$$Rf(s,\phi) = \int_{x_1 \cos\phi + x_2 \sin\phi = s} f(x)dx.$$

Here, $x \in \mathbb{R}$ and $(s, \phi) \in M = \mathbb{R} \times (-\pi, \pi)$. Note that because we are dealing with a local problem for Rf, it suffices to use local coordinates in the region of interest. We model the beam-hardening effects by a polynomial function $F : \mathbb{C} \to \mathbb{C}$ of the form

$$F(t) = \sum_{j=2}^{J} a_j t^j, \tag{4}$$

where a_j are constant, and $J \in \mathbb{N}$. Then the X-ray CT data is modeled by

$$P = Rf + P_{MA}, \quad P_{MA} = F(R\chi_D). \tag{5}$$

For the reconstruction, we apply the FBP to get

$$f_{CT} = f + f_{MA}, \quad f_{MA} = R^* \mathscr{I}^{-1} P_{MA}, \tag{6}$$

where $\mathscr{I}^{-1}$ is the Riesz potential, and R^* denotes the adjoint of R; see, for example, [16]. Our main result is as follows.

THEOREM 2.1. *Suppose $D_j, j = 1, 2$, are strictly convex. Then F in* (4) *is uniquely determined by f_{CT} in* (6).

Once F is determined, one can remove P_{MA} from P in (5) and reconstruct f. We remark that if $F(R\chi_D)$ has a linear part such as $a_0 + a_1 R\chi_D$, it could produce ambiguity in the reconstruction of f, although the term will not change the wave front set of f. We also remark that in the proof of Theorem 2.1, it suffices to use f_{CT} away from ∂D to determine F. So the theorem really says that F can be determined from the artifacts rather than the whole f_{CT}. This is important because f in (3) is singular at ∂D. The singularities of f_{MA} at ∂D are weaker, so it might be more difficult to recover F from those singularities. Among other things, one useful consequence is the following.

COROLLARY 2.2. *Under the assumption of Theorem* 2.1, *$f_{CT} \in C^\infty(\mathbb{R}^2 \backslash \partial D)$ if and only if $F = 0$.*

The result implies that the artifact is always visible unless there is no beam-hardening effect. This seems to be the first existence result for the streaking artifacts.

Next, we make a few remarks regarding the possible generalizations of the main results.

Remark 2.3 (the nonlinear function F). As studied in [12, 11, 19], the artifacts are generated from P_{MA} in (5) at certain discrete points. We will see in section 3 that near those points, it suffices to consider t small in (4). Thus, assuming F of the form (4) is not restrictive. In fact, one can consider variable coefficient polynomial $F(t, s, \phi) = \sum_{j=2}^{J} a_j(s, \phi) t^j$ as one would when α in f_E is not a constant; see equation (2.4) of [12]. We believe that our method can be adapted to recover $a_j(s, \phi)$ at those discrete points where artifacts are generated.

It is also natural to consider smooth nonlinear function $F(t)$ and recover coefficients of the Taylor expansion at $t = 0$. We believe that this is possible but requires further efforts. In particular, our method relies on the analysis of singularities in $F(R\chi_D)$, where $R\chi_D$ is a conormal distribution. The nonlinear interaction produces new singularities. For polynomial functions, we can describe the nature of the singularities within the framework of Lagrangian distributions. For smooth functions, the same applies to the truncated Taylor series, but it is not clear if the remainder term can be described in terms of Lagrangian distributions. One possible solution is to estimate the strength of new singularities in certain microlocal Sobolev spaces and

show that the remainder term is more regular. We refer the reader to [17] for an example of this approach.

Remark 2.4 (the number of objects). The streaking artifacts are associated with lines tangent to both D_1 and D_2. If the metal regions consist of more than two disjoint simply connected regions, our methods can be adapted to the case when there is no line tangent to more than two of the regions.

Remark 2.5 (the convexity assumption). The assumption that $D_j, j = 1, 2$, are strictly convex is essential. In section 4, we will show that $R\chi_{D_j}, j = 1, 2$, possess better regularity properties under the strict convexity assumption, which is key to determining F. The strict convexity can be relaxed to convexity of finite orders. We believe that the techniques developed in this paper are adaptable. However, if the boundary contains line segments, or the boundary is not smooth (e.g., contains corners), the generation of artifacts becomes more complicated as shown in [11]. It becomes unclear whether the nonlinear function can be recovered from the artifacts.

Finally, we briefly discuss the ideas of the proof. We already mentioned that streaking artifacts are associated with singularities, more precisely, wave front sets of $F(R\chi_D)$ due to the nonlinear interactions of the singularities in $R\chi_D$. With more precise notions of Lagrangian distributions, quantitative results on the strength of the artifacts are obtained in [11]; see also [19] for nonconvex objects. Essentially, these results provided the upper bound of the wave front set, which indicates where the artifact *could* appear. Our idea is that when the artifact *actually* occurs, it carries information about the nonlinear function F. So, we can use the artifact to reconstruct F. The philosophy that nonlinearity can help solve inverse problems was perhaps first demonstrated in [9] for nonlinear wave equations. In the last decade, the method has undergone rapid developments, and the majority of the work relies on the idea of higher order linearization. Unfortunately, this method is not applicable to our problem because it requires the X-ray data for a family of metal objects, but we only have one.

The way we overcome the difficulty is to study the fine structure of singularities in $F(R\chi_D)$. A key observation, discussed in section 4, is that when D is strictly convex, $R\chi_D$ is a conormal distribution vanishing to certain order at the singular support. This allows us to obtain expansion of $F(R\chi_D)$ near the interaction point in terms of the strength of singularities instead of the magnitudes in the higher order linearization expansion. To recover F, another key component is to show that all terms in the expansion are nontrivial. This is done in section 5, where we finish the proofs of Theorem 2.1 and Corollary 2.2.

3. Microlocal analysis of the artifacts. In this section, we consider the artifact generation for the special case of a quadratic nonlinearity. The analysis demonstrates some essential ingredients for proving Theorem 2.1. The other ingredients will be studied in section 4. We remark that some of the analysis already appeared in [11], but we need to improve them so they can be used for more general nonlinearities. Also, we introduce relevant notions from microlocal analysis along the way.

3.1. Regularity of $R\chi_D$. We start with the notion of conormal distributions; see section 18.2 of [5] for details. Let $\Omega \subset \mathbb{R}^n, n \in \mathbb{N}$, denote an open and relatively compact subset. Let $\Sigma \subset \Omega$ be a submanifold of codimension k. The set of conormal distributions of order m is denoted by $I^m(\Omega; \Sigma)$. Such distributions can be defined in a coordinate invariant way, but we only need the local representations. According to Theorem 18.2.8 of [5], $u \in I^m(\Omega; \Sigma)$ if and only if $u \in C^\infty(\mathbb{R}^n \setminus \Sigma)$, and near any

point $p \in \Sigma$ and in local coordinates where $\Sigma = \{y_1 = y_2 = \cdots = y_k = 0\}$, $y = (y', y'')$, $y' = (y_1, y_2, \ldots, y_k)$, $y'' \in \mathbb{R}^{n-k}$, we have

$$u(y) = \int_{\mathbb{R}^k} e^{iy'\cdot\eta'} a(\eta', y'')\, d\eta', \quad a \in S^{m+\frac{n-2k}{4}}(\mathbb{R}^k \times \mathbb{R}^{n-k}), \tag{7}$$

where for $r \in \mathbb{R}$, $S^r(\mathbb{R}^k \times \mathbb{R}^{n-k})$ is the class of symbols satisfying

$$|\partial_{y''}^{\alpha} \partial_{\eta'}^{\beta} a(\eta', y'')| \le C_{\alpha,\beta}(1 + |\eta'|)^{r-|\beta|}.$$

It is known that $\mathrm{WF}(u) \subset N^*\Sigma$ and the space of distributions satisfy

$$I^m(\Omega; \Sigma) \subset I^{m'}(\Omega; \Sigma), \quad m < m'.$$

The principal symbol of u is defined to be the equivalence class of $a(\eta', y'')$ in the quotient $S^{m+\frac{n-2k}{4}}(\mathbb{R}^k \times \mathbb{R}^{n-k})/S^{m+\frac{n-2k}{4}-1}(\mathbb{R}^k \times \mathbb{R}^{n-k})$, and the map

$$I^m(\Omega; \Sigma)/I^{m-1}(\Omega; \Sigma) \longrightarrow S^{m+\frac{n-2k}{4}}(\mathbb{R}^k \times \mathbb{R}^{n-k})/S^{m+\frac{n-2k}{4}-1}(\mathbb{R}^k \times \mathbb{R}^{n-k}),$$
$$[u] \longmapsto [a],$$

is an isomorphism. The symbol map can be invariantly defined as in [5], but since our analysis is completely local, we do not need to discuss that. It is worth mentioning that there is an equivalent definition of conormal distributions using iterated application of vector fields tangent toΣ; see Definition 18.2.6 of [5]. Then it is clear that such distributions belong to certain Besov spaces. Below, we mostly consider $n = 2$ and $k = 1$.

Let $D_j, j = 1, 2$, be a simply connected bounded domain in $\mathbb{R}^2$ with smooth strictly convex boundary ∂D_j. The characteristic function $\chi_{D_j} \in I^{-1}(\mathbb{R}^2; \partial D_j)$. It is known (see, for example, [11]) that $R\chi_{D_j} \in I^{-\frac{3}{2}}(M; S_j), j = 1, 2$. Also, we will see a direct calculation in section 3. But we give the proof below for the reader's convenience.

To describe the conormal distribution, we start with $R : \mathscr{E}'(\mathbb{R}^2) \to \mathscr{D}'(M)$ as an elliptic Fourier integral operator. Using local coordinates (s, ϕ) for M and $x = (x_1, x_2)$ for $\mathbb{R}^2$, we write the Schwartz kernel of R, denoted by K_R, as an oscillatory integral

$$K_R(s, \phi, x) = \frac{1}{(2\pi)^{\frac{1}{2}}} \int_{\mathbb{R}} e^{i(x_1 \cos\phi + x_2 \sin\phi - s)\lambda} d\lambda.$$

The phase function is $\phi(s, \phi, x; \lambda) = (x_1 \cos\phi + x_2 \sin\phi - s)\lambda$, so the associated Lagrangian submanifold of $T^*M \times T^*\mathbb{R}^2$ is

$$\Lambda = \{(x_1 \cos\phi + x_2 \sin\phi, \phi, -\lambda, \lambda(-x_1 \sin\phi + x_2 \cos\phi); x_1, x_2, \lambda\cos\phi, \lambda\sin\phi) : \\ \lambda \in \mathbb{R}\backslash 0, \phi \in (-\pi, \pi), x_1, x_2 \in \mathbb{R}\}.$$

In particular, $K_R \in I^{-\frac{1}{2}}(M \times \mathbb{R}^2; \Lambda)$. We denote the homogeneous canonical relation by

$$\begin{aligned} C = \{&(x_1 \cos\phi + x_2 \sin\phi, \phi, -\lambda, \lambda(-x_1 \sin\phi + x_2 \cos\phi); \\ &x_1, x_2, -\lambda\cos\phi, -\lambda\sin\phi) : \\ &\lambda \in \mathbb{R}\backslash 0, \phi \in (-\pi, \pi), x_1, x_2 \in \mathbb{R}\} \subset T^*M\backslash 0 \times T^*\mathbb{R}^2\backslash 0. \end{aligned} \tag{8}$$

Let $C_j \overset{\text{def}}{=} N^*\partial D_j\backslash 0, j = 1, 2$; we think of them as canonical relations of χ_{D_j} (see Appendix A). The composition of the two homogeneous canonical relations C, C_j is

transversal (see Appendix A) so the composition $C \circ C_j$ is a homogeneous canonical relation, which is a Lagrangian submanifold of T^*M. Under the strict convexity assumption, the Lagrangian becomes a conormal bundle. In fact, the projection of $C \circ C_j$ to M is injective, and the projection is

$$S_j \stackrel{\text{def}}{=} \{(s,\phi) \in M : s = x_1 \cos\phi + x_2 \sin\phi, \quad (x_1,x_2) \in \partial D_j, \\ (-\sin\phi, \cos\phi) \in T_{(x_1,x_2)} \partial D_j\}, \tag{9}$$

which consists of codimension one submanifolds of M. We have $C \circ C_j = N^* S_j \backslash 0, j = 1,2$. One can apply the FIO (Fourier integral operator) composition theorem [6, Theorem 25.2.3] to conclude that $R\chi_{D_j} \in I^{-\frac{3}{2}}(M; S_j), j = 1,2$.

3.2. The nonlinear analysis. We consider a quadratic nonlinearity $F(t) = t^2$ and let

$$\tilde{P}_{MA} \stackrel{\text{def}}{=} (R(\chi_D))^2 = (R(\chi_{D_1}))^2 + (R(\chi_{D_2}))^2 + 2R(\chi_{D_1})R(\chi_{D_2}). \tag{10}$$

We analyze the singularity in each term. For $(R\chi_{D_j})^2, j = 1,2$, we recall the following multiplicative property of conormal distributions; see [15].

LEMMA 3.1. *If $\Sigma \subset \Omega$ is a C^∞ hypersurface, and if $u, v \in I^{m-\frac{n}{4}+\frac{1}{2}}(\Omega; \Sigma)$ and $m < -1$, then $uv \in I^{m-\frac{n}{4}+\frac{1}{2}}(\Omega; \Sigma)$.*

We conclude that $(R\chi_{D_j})^2 \in I^{-\frac{3}{2}}(M; S_j), j = 1,2$. So, $\mathrm{WF}((R\chi_{D_j})^2) \subset N^* S_j$ does not produce new singularities.

Next, consider the product $R\chi_{D_1} R\chi_{D_2}$ in (10). This term will produce new singularities, and the result can be described by using the notion of paired Lagrangian distributions; see [3] for details. Let X be an n-dimensional manifold, $\Lambda_0, \Lambda_1 \subset T^*X \backslash 0$ be two cleanly intersecting Lagrangians in the sense that $\Sigma = \Lambda_0 \cap \Lambda_1$ is smooth, and $T_q\Sigma = T_q\Lambda_0 \cap T_q\Lambda_1, q \in \Sigma$. The paired Lagrangian distributions associated with the pair (Λ_0, Λ_1) with order $p, l \in \mathbb{R}$ is denoted by $I^{p,l}(\Lambda_0, \Lambda_1)$. We only need the case when Λ_0, Λ_1 are conormal bundles. Locally, such distributions can be described as follows; see [2]. Let $x = (x_1, \ldots, x_n)$ be coordinates of $\mathbb{R}^n$. Let $k_1, k_2 \in \mathbb{N}$ and $k_1 + k_2 = n$. Consider

$$Y_1 = \{x_1 = x_2 = \cdots x_{k_1} = 0\} = \{x' = 0\}, \\ Y_2 = \{x_1 = x_2 = \cdots x_{k_1+k_2} = 0\} = \{x' = 0, x'' = 0\}.$$

Let $\Lambda_0 = N^* Y_1 \backslash 0, \Lambda_1 = N^* Y_2 \backslash 0$ and $u \in I^{p,l}(\Lambda_0, \Lambda_1)$ be written as

$$u(x) = \int_{\mathbb{R}^{k_1+k_2}} e^{i(x' \cdot \xi' + x'' \cdot \xi'')} a(x, \xi', \xi'') d\xi' d\xi'', \tag{11}$$

with $a(x; \xi', \xi'')$ belonging to the product type symbols

$$S^{\mu,\mu'}(\mathbb{R}^n \times (\mathbb{R}^{k_1} \backslash 0) \times \mathbb{R}^{k_2}) = \{a \in C^\infty : |\partial_x^\gamma \partial_{\xi''}^\beta \partial_{\xi'}^\alpha a(x,\xi)| \\ \le C_{\alpha\beta\gamma K} \langle \xi', \xi'' \rangle^{\mu - |\alpha|} \langle \xi'' \rangle^{\mu' - |\beta|}\}, \tag{12}$$

where $\mu = p - k_1/2 + n/4, \mu' = l - k_2/2$. We recall the fact that if $u \in I^{p,l}(\Lambda_0, \Lambda_1)$, then $\mathrm{WF}(u) \subset \Lambda_0 \cup \Lambda_1$. Also, near $\Lambda_0 \backslash \Lambda_1$, u is microlocally in $I^{p+l}(\Lambda_0)$. More precisely, for any open sets U_1, U_2 in $T^*X \backslash 0$ such that $\Lambda_1 \subset U_1 \subset U_2$, let χ be a smooth real function on T^*X with values in $[0,1]$ such that $\chi = 0$ on U_1 and $\chi = 1$ on $\Lambda_0 \backslash U_2$. Then $\tilde{u}$ with amplitude χa as in (11) is a Lagrangian distribution in $I^{p+l}(\Lambda_0)$. For

convenience, we refer to this type of statement as $u \in I^{p+l}(\Lambda_0 \backslash \Lambda_1)$. Similarly, for $u \in I^{p,l}(\Lambda_0, \Lambda_1)$, we have $u \in I^p(\Lambda_1 \backslash \Lambda_0)$. Thus the principal symbols can be defined invariantly for each piece. In fact, one can also define the notion of principal symbols for u invariantly; see [3]. However, we only need the behavior of these distributions locally. So, it suffices to work with the expression (11).

To analyze the singularities in $R\chi_{D_1} R\chi_{D_2}$, we need to know how the Lagrangians intersect. As shown in [11], if D_1, D_2 are strictly convex, then S_1 intersect S_2 transversally at a finite point set $S_\diamond = S_1 \cap S_2$; see Figure 1.

LEMMA 3.2. *For each $q \in S_\diamond$, there exists neighborhood O of q such that in O,*

$$R(\chi_{D_1}) R(\chi_{D_2}) \in I^{-\frac{3}{2},-1}(T_q^* M, N^* S_1) + I^{-\frac{3}{2},-1}(T_q^* M, N^* S_2). \tag{13}$$

Moreover, $R(\chi_{D_1}) R(\chi_{D_2}) \in I^{-5/2}(T_q^* M \backslash (N^* S_1 \cup N^* S_2))$, and the principal symbol is nonvanishing.

Proof. We repeat the proof of Lemma 1.1 of [2]. Consider the intersection of S_1, S_2 at q. We choose local coordinates (x_1, x_2) for $\mathbb{R}^2$ such that $q = (0,0)$, $S_1 = \{x_1 = 0\}$, and $S_2 = \{x_2 = 0\}$. Then we can write

$$R\chi_{D_1}(x) = \int_{\mathbb{R}} e^{ix_1\xi_1} a(x, \xi_1) d\xi_1, \quad a \in S^{-3/2}(\mathbb{R}^2_x \times (\mathbb{R}_{\xi_1} \backslash 0)),$$
$$R\chi_{D_2}(x) = \int_{\mathbb{R}} e^{ix_2\xi_2} b(x, \xi_2) d\xi_2, \quad b \in S^{-3/2}(\mathbb{R}^2_x \times (\mathbb{R}_{\xi_2} \backslash 0)),$$

and the principal symbols of a, b are nonvanishing. Then we get

$$R\chi_{D_1}(x) R\chi_{D_2}(x) = \int_{\mathbb{R}} \int_{\mathbb{R}} e^{ix_1\xi_1 + ix_2\xi_2} a(x, \xi_1) b(x, \xi_2) d\xi_1 d\xi_2. \tag{14}$$

Introduce a cutoff function $\chi(t) \in C_0^\infty(\mathbb{R})$, $\chi = 1$ for $|t| \le 1/2$ and $\chi = 0$ for $|t| \ge 2$. Then we have

$$\begin{aligned} &\chi(\langle \xi_2 \rangle / \langle \xi_1 \rangle) a(x, \xi_1) b(x, \xi_2) \in S^{-3/2,-3/2}(\mathbb{R}^2_x \times (\mathbb{R}_{\xi_2} \backslash 0) \times \mathbb{R}_{\xi_1}), \\ &(1 - \chi)(\langle \xi_2 \rangle / \langle \xi_1 \rangle) a(x, \xi_1) b(x, \xi_2) \in S^{-3/2,-3/2}(\mathbb{R}^2_x \times (\mathbb{R}_{\xi_1} \backslash 0) \times \mathbb{R}_{\xi_2}) \end{aligned} \tag{15}$$

by directly checking that the symbols satisfy the product type estimate in (12). For example, let's consider the first term in (15). For $\alpha, \beta \in \mathbb{N}$, $\gamma \in \mathbb{N}^2$ and on a compact set of $\mathbb{R}^2_x$, we have

$$\begin{aligned} |\partial_x^\gamma \partial_{\xi_1}^\alpha \partial_{\xi_2}^\beta (\chi(\langle \xi_2 \rangle / \langle \xi_1 \rangle) a(x, \xi_1) b(x, \xi_2))| &\le C_{\alpha\beta\gamma} \langle \xi_1 \rangle^{-3/2-\alpha} \langle \xi_2 \rangle^{-3/2-\beta} \\ &\le C_{\alpha\beta\gamma} \langle (\xi_1, \xi_2) \rangle^{-3/2-\alpha} \langle \xi_2 \rangle^{-3/2-\beta}, \end{aligned}$$

where we used the facts that this term is supported in $\langle \xi_2 \rangle \le 2\langle \xi_1 \rangle$ and $C_{\alpha\beta\gamma}$ is a generic constant. Thus this is a symbol of a paired Lagrangian distribution in $I^{p,l}(T_q^* M, N^* S_2)$, where the orders are $p = -3/2 + 1/2 - 1/2 = -3/2$ and $l = -3/2 + 1/2 = -1$.

To find the principal symbol on $T_q^* M \backslash (N^* S_1 \cup N^* S_2)$, we consider (14) for $C_1 \langle \xi_2 \rangle \le \langle \xi_1 \rangle \le C_2 \langle \xi_2 \rangle$ for some positive constants C_1, C_2. Then the symbol $ab \in S^{-3}(\mathbb{R}^2 \times \mathbb{R}^2)$ and the principal symbol is given by the product of principal symbols of a and b. ∎

To summarize, we prove the following.

LEMMA 3.3. *Suppose D_1, D_2 are strictly convex. Then for $\tilde{P}_{MA}$ defined in* (10)*, we have $WF(\tilde{P}_{MA}) \subset (\cup_{q\in S_\diamond} T^*_q M) \cup N^*S_1 \cup N^*S_2$. Moreover, $(\cup_{q\in S_\diamond} T^*_q M)\backslash(N^*S_1 \cup N^*S_2) \subset WF(\tilde{P}_{MA})$.*

3.3. Description of the artifact. Consider $\tilde{f}_{MA} \overset{\text{def}}{=} R^*\mathscr{I}^{-1}(R\chi_D)^2$. We show that this term contributes to the streaking artifacts. We define $L_\diamond = \{L : L$ is a straight line in $\mathbb{R}^2$ tangent to D_1 and $D_2\}$.

LEMMA 3.4. *Fix any $L \in L_\diamond, p \in L$, and let $\chi \in C_0^\infty(\mathbb{R}^2)$ be supported near p and away from $\partial D_1 \cup \partial D_2 \cup (\cup_{\tilde{L}\in L_\diamond, \tilde{L}\neq L} \tilde{L})$. Then we have $\chi\tilde{f}_{MA} \in I^{-2}(N^*L)$, and the principal symbol is nonvanishing.*

Proof. Essentially, $\mathscr{I}^{-1}$ can be regarded as a pseudodifferential operator of order 1 (modulo a smoothing operator); see, for instance, the treatment of Lemma 4.1 of [19]. Also, we know that R^* is an elliptic FIO of order $-\frac{1}{2}$. Let C^* be the canonical relation of R^*. Then we check that $C^* \circ N^*S_j\backslash 0 = C^* \circ C \circ N^*\partial D_j\backslash 0 = N^*\partial D_j\backslash 0, j = 1, 2$. It follows from the wave front analysis that

$$\mathrm{WF}(R^*\mathscr{I}^{-1}((R\chi_{D_j}))^2) \subset N^*\partial D_j, \quad j = 1, 2.$$

Next, consider singularities in $R^*\mathscr{I}^{-1}(R\chi_{D_1}R\chi_{D_2})$. First, for $q \in S_\diamond$ and letting χ_q be a smooth cut-off function supported near q, we have

$$\mathscr{I}^{-1}\big(\chi_q R(\chi_{D_1})R(\chi_{D_2})\big) \in I^{-\frac{1}{2},-1}(T^*_q M, N^*S_1) + I^{-\frac{1}{2},-1}(T^*_q M, N^*S_2),$$

and the principal symbol at $T^*_q M\backslash(N^*S_1 \cup N^*S_2)$ is nonvanishing. Here, we used Proposition 4.1 of [3]. For the application of R^*, we can still use Proposition 4.1 of [3]. The transversality of the compositions $C^* \circ (T^*_q M\backslash 0)$ and $C^* \circ (N^*S_j\backslash 0), j = 1, 2$, are verified in Appendix A. In particular, $C^* \circ (T^*_q M\backslash 0) = N^*L\backslash 0$, where

$$L = \{x \in \mathbb{R}^2 : x_1 \cos\phi + x_2 \sin\phi = s, q = (s, \phi)\} \in L_\diamond.$$

So, we get

$$R^* \circ \mathscr{I}^{-1}\big(\chi_q R(\chi_{D_1})R(\chi_{D_2})\big) \in I^{-1,-1}(N^*L, N^*\partial D_1) + I^{-1,-1}(N^*L, N^*\partial D_2).$$

The principal symbol at $N^*L\backslash(N^*\partial D_1 \cup N^*\partial D_2)$ is the product of the principal symbols of $R^*\mathscr{I}^{-1}$ and $\chi_q R(\chi_{D_1})R(\chi_{D_2})$ at N^*L, so it is nonvanishing. The analysis can be repeated for each $q \in S_\diamond$, and the proof is completed. ∎

According to [12, Definition 3.2], the straight lines in $L_\diamond$ are *streaking artifacts* in the sense of wave front sets. Lemma 3.4 states that such artifacts always exist, namely $\mathrm{singsupp}(\tilde{f}_{MA})\backslash\partial D \neq \emptyset$ if the nonlinear function F is quadratic.

4. Improved regularity analysis. To analyze the singularities produced by higher order polynomial nonlinearities, we will use a special property of the Radon transform of χ_D when D is strictly convex. We start with Piriou's conormal distributions; see [15]. We remark that this notion will not be used in any essential way afterwards, but it provides a good motivation.

DEFINITION 4.1. *If $m < -1$, let $k(m)$ be the nonnegative integer such that $-m - 2 \le k(m) < -m - 1$. If $\Sigma \subset \Omega$ is a C^∞ hypersurface, we say that $u \in \overset{o}{I}{}^{m-\frac{n}{4}+\frac{1}{2}}(\Omega; \Sigma)$ if $u \in I^{m-\frac{n}{4}+\frac{1}{2}}(\Omega; \Sigma)$ vanishes to order $k(m)+1$ at Σ (all derivatives of u to order less than or equal to $k(m)$ vanish atΣ).*

It is proved in Proposition 2.4 of [18] that if $\Sigma \subset \Omega$ is a C^∞ hypersurface, $u \in I^{m-\frac{n}{4}+\frac{1}{2}}(\Omega;\Sigma)$, and $m<-1$, then $u=\mathscr{E}+v$, with $v \in \overset{o}{I}{}^{m-\frac{n}{4}+\frac{1}{2}}(\Omega;\Sigma)$ and $\mathscr{E} \in C^\infty$. If $v \in \overset{o}{I}{}^{m-\frac{n}{4}+\frac{1}{2}}(\Omega;\Sigma)$ and $\Sigma=\{y_1=0\}$, then $v=y_1^{k(m)}w$, $w \in I^{m+k(m)-\frac{n}{4}+\frac{1}{2}}(\Omega;\Sigma)$. Now consider $n=2$ and take $v \in \overset{o}{I}{}^{m}(\Omega;\Sigma), m<-1$. Then $v \in y_1^{k(m)} I^{m+k(m)}(\Omega;\Sigma)$. But since $m+k(m)<-1$, we get that

$$v^2 \in y_1^{2k(m)} I^{m+k(m)}(\Omega;\Sigma).$$

We can apply Proposition 18.2.3 of [5] to conclude that $v^2 \in I^{m-k(m)}(\Omega;\Sigma)$. The argument can be repeated to yield that for $l \in \mathbb{N}$, $v^l \in I^{m-(l-1)k(m)}(\Omega;\Sigma)$. In conclusion, if $k(m)>0$, the conormal distribution becomes more and more regular after self-multiplication. We observe that the vanishing order in Piriou's conormal distribution plays an important role in the argument.

Now let U be a simply connected bounded domain with smooth boundary ∂U. As in (9), let $S \overset{\text{def}}{=} \{(s,\phi) \in M : s=x_1\cos\phi+x_2\sin\phi, x \in \partial U, (-\sin\phi,\cos\phi) \in T_x\partial U\}$, which is a codimension one submanifold of M. We know that $R\chi_U \in I^{-\frac{3}{2}}(\mathbb{R}^2;S)$, so $m=-3/2$ and $k(m)=0$. It seems that we do not gain any vanishing order from the analysis above. However, if U is strictly convex, we show below that it is possible to gain $1/2$ vanishing order. We remark that for nonconvex domain, this is not true. One can construct simple examples to verify it; see Figure 2. It is also worth mentioning that the vanishing order is closely related to the range characterization for R, R^* and R^*R (in our notation) studied in section 4 of [10].

Below, we use $t_+^\alpha, \alpha>-1$, to denote homogeneous distributions so that $t_+^\alpha = t^\alpha$ for $t \geq 0$ and $t_+^\alpha = 0$ for $t<0$. See section 3.2 of [4] for details. Also, the Fourier transform of t_+^α is homogeneous of degree $-\alpha-1$; see Theorem 7.1.16 of [4]. The key result of this section is the following.

LEMMA 4.2. *Suppose U is strictly convex. For $q_0 \in S$, there exists a neighborhood of q_0 and local coordinates $y=(y_1,y_2) \in \mathbb{R}^2$ such that $q_0=(0,0)$, $S=\{y_2=0\}$, and*

$$R\chi_U(y) = h(y)y_{2,+}^{1/2} + y_{2,+}r(y), \quad r \in I^{-3/2}(M;S),$$

where h is smooth and positive.

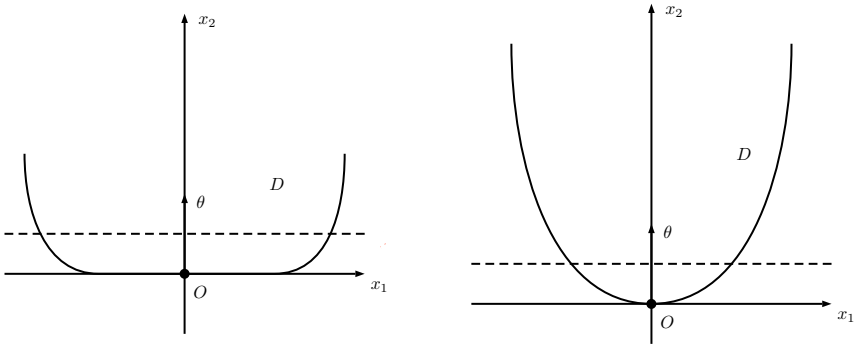

FIG. 2. *Regularity of $R\chi_D(s,\theta)$. We consider θ in the direction of the x_2-axis. Then $R\chi_D(s,\theta)$ is the integration of $\chi_D(x)$ along the dashed line with distance s to the x_1-axis. Left figure: D is not strictly convex near O. $R\chi_D(s,\theta)$ has a Heaviside type singularity in s. Right figure: D is strictly convex near O. Then $R\chi_D(s,\theta)$ behaves like a homogeneous distribution $s_+^{1/2}$ in s.*

Note that $y_{2,+} \in I^{-3/2}(M;S)$, so the product $y_{2,+}r(y)$ makes sense as a product of distributions in $I^{-3/2}(M;S)$ by Lemma 3.1. Also, from the local expression (7), we see that $I^{-3/2}(M;S) \subset L^\infty$; see also [2]. So, the product also makes sense in L^∞.

Proof. Consider the Radon transform

$$R\chi_U(s,\phi) = \int_{s=x_1\cos\phi + x_2\sin\phi} \chi_U(x_1,x_2)dx_1dx_2. \tag{16}$$

As pointed out by a referee, we have a simple interpretation that $R\chi_U$ is the length of the line segment contained in U. We can compute it in a conveniently chosen coordinate system.

Recall that ∂U is a simple closed strictly convex curve if and only if the curvature κ is strictly positive on ∂U; see section 2.3 of [8]. Here, the curvature is defined in the Frenet frame and is always nonnegative. For any ϕ, we let $p = (p_1, p_2)$ be a point on ∂U such that $\theta = (\cos\phi, \sin\phi)$ is orthogonal to $T_q(\partial U)$. (By the strict convexity of U, there are two points with this property which can be distinguished by the value $s_0 = p_1\cos\phi + p_2\sin\phi$.) We compute the integral in (16) in the Frenet frame at p. Thus, we choose local coordinates (z_1, z_2) near p such that $p = (0,0)$, and the z_1-axis is tangent to ∂U at p. Moreover, by selecting the orientation of ∂U, we can arrange the new coordinate system to have the same orientation as the original one, and U stays in $z_2 > 0$. Let $\Phi : \mathbb{R}^2 \to \mathbb{R}^2$ be the coordinate change so that $z = \Phi(x;\phi)$. Note that $\Phi(\bullet;\phi)$ locally depends on ϕ smoothly. Also, we find that $dx = J(z;\phi)dz$, where J is the Jacobian factor and $J = 1$. Note that in this new coordinate system, we have $s = x_1\cos\phi + x_2\sin\phi = s_0 \pm z_2$, where the sign is $+$ if θ is in the direction of the positive z_2-axis and $-$ otherwise. It suffices to consider $+$ below because the other case is identical. Thus (16) becomes

$$R\chi_U(s,\phi) = \int_{\mathbb{R}} \chi_U(z_1, s - s_0)dz_1. \tag{17}$$

Suppose ∂U is parametrized by arc-length τ starting from q. Then in the Frenet frame, we have the canonical form of the curve

$$z_1(\tau) = \tau - \frac{\kappa^2\tau^3}{6} + o(\tau^3), \quad z_2(\tau) = \frac{\kappa}{2}\tau^2 + \frac{\kappa'\tau^3}{6} + o(\tau^3);$$

see section 1-6 of [1]. Here, κ, κ' are the curvature and its τ derivative at q. As $\kappa > 0$, by using the inverse function theorem, we can take $z_1 \in (-\delta, \delta)$ with $\delta > 0$ small as the parameter and express the curve as the graph of a function

$$z_2 = \frac{\kappa}{2}z_1^2 + \frac{\kappa' z_1^3}{6} + o(z_1^3).$$

For $z_2 > 0$ close to 0, we have two roots $z_{1,\pm}$ given by

$$z_{1,+} = \left(\frac{2}{\kappa}\right)^{\frac{1}{2}} z_2^{\frac{1}{2}} + a_{2,+}z_2 + \cdots; \quad z_{1,-} = -\left(\frac{2}{\kappa}\right)^{\frac{1}{2}} z_2^{\frac{1}{2}} + a_{2,-}z_2 + \cdots.$$

Finally, we use $z_2 = s - s_0$ to get

$$\begin{aligned} R\chi_D(s,\phi) &= z_{1,+} - z_{1,-} \\ &= 2\left(\frac{2}{\kappa}\right)^{\frac{1}{2}} (s-s_0)_+^{\frac{1}{2}} + c_2(s-s_0)_+ + \cdots. \end{aligned} \tag{18}$$

For ϕ sufficiently close to some ϕ_0, we note that s, s_0, and the coefficients of $(s-s_0)_+^a$ in (18) depend on ϕ smoothly. The proof is completed after a change of variable $y_2 = s - s_0, y_1 = \phi - \phi_0$. ∎

Next, we consider the situation near $S_\diamond$.

LEMMA 4.3. *Suppose D_1, D_2 are strictly convex. For $q_0 \in S_1 \cap S_2$, there are local coordinates $y = (y_1, y_2) \in \mathbb{R}^2$ near q_0 such that locally $q_0 = (0,0)$, $S_1 = \{y_2 = 0\}, S_2 = \{y_1 = 0\}$, and*

$$R\chi_{D_1}(y) = h_1(y) y_{2,+}^{1/2} + y_{2,+} r_1(y), \quad r_1 \in I^{-3/2}(M; S_1),$$
$$R\chi_{D_2}(y) = h_2(y) y_{1,+}^{1/2} + y_{1,+} r_2(y), \quad r_2 \in I^{-3/2}(M; S_2),$$

where $h_j, j = 1, 2$ are smooth and positive.

Proof. First, we apply Lemma 4.2 to find a neighborhood V_1 of q_0 and coordinates (z_1, z_2) such that $S_1 = \{z_2 = 0\}$. Then we apply Lemma 4.2 again to find a neighborhood V_2 of q_0 and coordinates (w_1, w_2) such that $S_2 = \{w_2 = 0\}$. Because S_1 intersects S_2 transversally at q_0 (see [11]), we know that the z_2-axis is not parallel to the w_2-axis. Thus, we can find a new coordinate system (y_1, y_2) with $y_1 = z_2$, $y_2 = w_2$. Then we write $z_1 = z_1(y), w_1 = w_1(y)$ as smooth functions. Finally, the conclusions follow from Lemma 4.2. ∎

The vanishing order is the key to obtaining multiplicative properties similar to Piriou's distributions.

LEMMA 4.4. *Let $m, n \in \mathbb{N}$. Under the assumptions of Lemma 4.3, we have*

1. *$(R\chi_{D_1})^n(y) = h_1(y) y_{2,+}^{n/2} + y_{2,+}^{(1+n)/2} r_1(y)$ and $(R\chi_{D_2})^n(y) = h_2(y) y_{1,+}^{n/2} + y_{1,+}^{(1+n)/2} r_2(y)$, where $r_j \in I^{-3/2}(M; S_j), j = 1, 2$, and h_j are smooth and positive.*
2. *$(R\chi_{D_1})^m(y)(R\chi_{D_2})^n(y) = h(y) y_{2,+}^{m/2} y_{1,+}^{n/2} + r(y)$, where r is a sum of paired Lagrangian distributions such that $r \in I^{-2-m/2-n/2}(T^*_{q_0} M \backslash (N^* S_1 \cup N^* S_2))$, and h is smooth and positive.*

Proof. (1) We prove the case for $n = 2$. The general case can be obtained by induction. Also, it suffices to consider $R\chi_{D_1}$. The analysis for $R\chi_{D_2}$ is similar. We can find a proper coordinate as in Lemma 4.3 and write

$$R\chi_{D_1}(y) = \tilde{h}_1(y) y_{2,+}^{1/2} + y_{2,+} \tilde{r}_1(y), \quad \tilde{r}_1 \in I^{-3/2}(M; S_1).$$

Then

$$(R\chi_{D_1})^2 = \tilde{h}_1^2(y) y_{2,+} + 2\tilde{h}_1(y)\tilde{r}_1(y) y_{2,+}^{3/2} + y_{2,+}^2 \tilde{r}_1^2(y).$$

Note that $\tilde{h}_1 \tilde{r}_1 \in I^{-3/2}(M; S_1)$. Also, $\tilde{r}_1^2 \in I^{-3/2}(M; S_1)$, so $y_{2,+}^{\frac{1}{2}} \tilde{r}_1^2 \in I^{-3/2}(M; S_1)$ as well.

(2) We use the coordinates in Lemma 4.3 and part (1) to get

$$(R\chi_{D_1})^m(y) = h_1(y) y_{2,+}^{m/2} + y_{2,+}^{(1+m)/2} r_1(y), \quad r_1 \in I^{-3/2}(M; S_1),$$
$$(R\chi_{D_2})^n(y) = h_2(y) y_{1,+}^{n/2} + y_{1,+}^{(1+n)/2} r_2(y), \quad r_2 \in I^{-3/2}(M; S_2),$$

where h_1, h_2 are smooth and positive functions. Thus

$$(R\chi_{D_1})^m(y)(R\chi_{D_2})^n(y) = h_1(y)h_2(y) y_{2,+}^{m/2} y_{1,+}^{n/2} + h_1(y) r_2(y) y_{2,+}^{m/2} y_{1,+}^{(1+n)/2} + h_2(y) r_1(y) y_{1,+}^{n/2} y_{2,+}^{(1+m)/2} + y_{2,+}^{(1+m)/2} y_{1,+}^{(1+n)/2} r_1(y) r_2(y).$$

Note that $h_1 r_2 \in I^{-3/2}(M; S_2)$. In fact, from the proof of Lemma 4.3, we know that r_2 has an asymptotic expansion in $y_{2,+}^{\frac{1}{2}}$. Thus we see that $h_1(y) r_2(y) y_{2,+}^{m/2} \in I^{-1-m/2}(M; S_2)$. By using the proof of Lemma 3.2 (here, we need the result for different orders, but the proof is the same; see also [2]), we get

$$\begin{aligned} h_1(y) r_2(y) y_{2,+}^{m/2} y_{1,+}^{(1+n)/2} \in\ & I^{-1-m/2,-1-n/2}(T^*_{q_0} M, N^* S_2) \\ & + I^{-3/2-n/2,-1/2-m/2}(T^*_{q_0} M, N^* S_1). \end{aligned} \tag{19}$$

Similarly, we obtain that

$$\begin{aligned} h_2(y) r_1(y) y_{1,+}^{n/2} y_{2,+}^{(1+m)/2} \in\ & I^{-1-n/2,-1-m/2}(T^*_{q_0} M, N^* S_1) \\ & + I^{-3/2-m/2,-1/2-n/2}(T^*_{q_0} M, N^* S_2), \\ y_{2,+}^{(1+m)/2} y_{1,+}^{(1+n)/2} r_1(y) r_2(y) \in\ & I^{-3/2-n/2,-1-m/2}(T^*_{q_0} M, N^* S_1) \\ & + I^{-3/2-m/2,-1-n/2}(T^*_{q_0} M, N^* S_2). \end{aligned} \tag{20}$$

We conclude that microlocally away from $N^* S_1 \cup N^* S_2$, terms in (19) and (20) belong to $I^{-2-m/2-n/2}(T^*_{q_0} M)$. This completes the proof. ∎

5. Determination of the nonlinear term.

Proof of Theorem 2.1. Suppose $\tilde{F}(t) = \sum_{j=2}^{\tilde{J}} \tilde{a}_j t^j$ is another nonlinear polynomial of the form (4). Let $\tilde{P}_{MA}, \tilde{f}_{CT}$ be the corresponding functions for $\tilde{F}$. Assume that $f_{CT} = \tilde{f}_{CT}$. We consider

$$P_{MA} - \tilde{P}_{MA} = \sum_{j=2}^{J} (a_j - \tilde{a}_j)(R\chi_D)^j. \tag{21}$$

Here, we assumed $J \geq \tilde{J}$, and we let $\tilde{a}_j = 0$ for $j > \tilde{J}$. We claim that for any $q \in S_\diamond$,

$$\mathrm{WF}(P_{MA} - \tilde{P}_{MA}) \cap (T^*_q M \backslash (N^* S_1 \cup N^* S_2)) = \emptyset. \tag{22}$$

To see this, we first use the analysis in section 3.1 and Lemma 3.2 (see also Lemma 4.4) to conclude that $P_{MA} - \tilde{P}_{MA}$ is a sum of paired Lagrangian distributions in

$$I^{a,b}(T^*_q M, N^* S_1) + I^{a',b'}(T^*_q M, N^* S_2),$$

where we did not find the orders a, a', b, b' because they are not important for this argument. Let u be the sum of terms such that $u \in I^c(T^*_q M \backslash (N^* S_1 \cup N^* S_2))$ with $c = \max(a+b, a'+b')$. If $c = -\infty$, we are done. Otherwise, c is a finite number, and the principal symbol of u on $T^*_q M \backslash (N^* S_1 \cup N^* S_2)$ is nonvanishing. We can repeat the proof of Lemma 3.4 line by line, and the symbol calculation in Lemma 3.4 yields a contradiction because $f_{CT} - \tilde{f}_{CT}$ is smooth away from ∂D.

Next, we show that $a_j = \tilde{a}_j$ in (21). Without loss of generality, we can take $\tilde{a}_j = 0$ and show $a_j = 0$. We expand and regroup the terms in (21) as

$$\begin{aligned} & \sum_{j=2}^{J} a_j (R\chi_D)^j = \sum_{j=2}^{J} a_j (R\chi_{D_1})^j + \sum_{j=2}^{J} a_j (R\chi_{D_2})^j + \sum_{j=2}^{J} a_j A_j \\ & \text{where } A_j = \sum_{m+n=j, m,n \geq 1} C_{m,n} (R\chi_{D_1})^m (R\chi_{D_2})^n, \quad C_{m,n} > 0. \end{aligned}$$

To determine a_j, we use singularities at T_q^*M for $q \in S_\diamond$ away from $N^*S_1 \cup N^*S_2$, so it suffices to look at singularities in A_j. According to Lemma 4.4, we know that

$$A_j = \sum_{m+n=j,m,n\geq 1} C_{m,n} h_{m,n}(y) y_{2,+}^{m/2} y_{1,+}^{n/2} + r_{m,n}(y),$$

where $C_{m,n}$ and $h_{m,n}$ are both positive. Note that

$$C_{m,n} h_{m,n}(y) y_{2,+}^{m/2} y_{1,+}^{n/2} \in I^{-3/2-m/2-n/2}(T_q^*M \backslash (N^*S_1 \cup N^*S_2)).$$

We know from Lemma 4.4 that $r_{m,n} \in I^{-2-m/2-n/2}(T_q^*M \backslash (N^*S_1 \cup N^*S_2))$. Thus $A_j \in I^{-3/2-j/2}(T_q^*M \backslash (N^*S_1 \cup N^*S_2))$ and $r_{m,n}$ do not contribute to the leading order term.

To see that the principal symbol is nonvanishing, it suffices to find the Fourier transform of $A_{j,0} = \sum_{m+n=j,m,n\geq 1} C_{m,n} h_{m,n}(0) y_{2,+}^{m/2} y_{1,+}^{n/2} \chi(y_2)\chi(y_1)$, where $\chi(t), t \in \mathbb{R}$, is any smooth cut-off function equal to 1 near $t = 0$. We will choose $\chi(t)$ below. Note that $C_{m,n}, h_{m,n}(0)$ are all positive. It suffices to look at the Fourier transform of $\chi(t)t_+^a, a > 0$. First, we use the computation in Example 7.1.17 of [4] and consider the Fourier transform of $e^{-\epsilon t} t_+^a$ for $\epsilon > 0$ small, which is given by

$$(\epsilon + i\tau)^{-a-1} \int_0^\infty t^a e^{-t} dt.$$

Note that this is a nonvanishing symbol of order $-a-1$. Now we can approximate $e^{-\epsilon t}$ (extended to a Schwartz function on $\mathbb{R}$) by some $\chi \in C_0^\infty(\mathbb{R})$ equal to 1 near 0 and conclude that the Fourier transform of $\chi(t)t_+^a$ is a nonvanishing symbol of order $-a-1$. Applying the procedure to the terms in $A_{j,0}$, we conclude that the principal symbol of A_j on $T_q^*M \backslash (N^*S_1 \cup N^*S_2)$ is nonvanishing.

Now we can finish the proof. For $j = 2$, we get that $A_2 \in I^{-5/2}(T_q^*M \backslash (N^*S_1 \cup N^*S_2))$ and $A_j \in I^{-3}(T_q^*M \backslash (N^*S_1 \cup N^*S_2))$ for $j \geq 3$. Because the principal symbol of A_2 is nonvanishing, we derive from the claim in the beginning of the proof that $a_2 = 0$. Now we can repeat the argument for $j = 3, \ldots, J$ to get that all $a_j = 0$. This finishes the proof. ∎

Proof of Corollary 2.2. If $F = 0$, it is easy to see from (6) that $f_{CT} \in C^\infty(\mathbb{R}^2 \backslash \partial D)$. If $f_{CT} \in C^\infty$ away from ∂D, we know from the proof of Theorem 2.1 that (22) holds true for $\tilde{P}_{MA} = 0$ and $\tilde{a}_j = 0, j = 1, 2, \ldots, J$. Then the proof of Theorem 2.1 implies that $F = 0$. ∎

Appendix A. Composition of FIOs. The purpose of this appendix is to verify some technical conditions for the composition of Fourier integral operators in section 3. In particular, we check that the compositions of canonical relations in section 3.1 and Lemma 3.4 are transversal and proper.

We first recall the relevant definitions from [6, section 25.2]. Let X, Y, Z be three manifolds. Let C_1 be a homogeneous canonical relation from $T^*Y \backslash 0$ to $T^*X \backslash 0$, and let C_2 be a homogeneous canonical relation from $T^*Z \backslash 0$ to $T^*Y \backslash 0$; we say that the composition $C_2 \circ C_1$ is transversal if $\mathscr{X} = C_1 \times C_2$ intersects $\mathscr{Y} = T^*X \times \Delta(T^*Y) \times T^*Z$ transversally, that is, for any q in the intersection,

$$T_q\mathscr{X} + T_q\mathscr{Y} = T_q\mathscr{Z} \text{ with } \mathscr{Z} = T^*X \times T^*Y \times T^*Y \times T^*Z.$$

Here, $\Delta(T^*Y)$ denotes the diagonal set of $T^*Y \times T^*Y$. The composition is proper if the map $\mathscr{X} \cap \mathscr{Y} \to T^*(X \times Z) \backslash 0$ is proper. If the composition is transversal and

proper, then $C = C_2 \circ C_1$ is a canonical relation. We have Theorem 25.2.3 of [6] for the composition of FIOs. Actually, we only need the special case of transversal compositions. For the study of the composition of Fourier integral operators and conormal distributions, we take Z to be a point; see the treatment on page 22 of [6].

We start with the composition of C and $C_j, j = 1, 2$, in section 3.1. Recall from (8) that the canonical relation of R is parametrized as

$$\begin{aligned} C = \{&(x_1 \cos\phi + x_2 \sin\phi, \phi, -\lambda, \lambda(-x_1 \sin\phi + x_2 \cos\phi); \\ &x_1, x_2, -\lambda\cos\phi, -\lambda\sin\phi) : \\ &\lambda \in \mathbb{R}\backslash 0, \phi \in (-\pi, \pi), x_1, x_2 \in \mathbb{R}\} \subset T^*M\backslash 0 \times T^*\mathbb{R}^2\backslash 0. \end{aligned}$$

For $C_j = N^*\partial D_j\backslash 0, j = 1, 2$, we choose local coordinates (y_1, y_2) near $q \in \partial D_j$ such that $q = 0$ and $\partial D_j = \{y_2 = 0\}$. Then $C_j = \{(y_1, 0, 0, \xi_2) : y_1 \in \mathbb{R}, \xi_2 \in \mathbb{R}\backslash 0\}$. Now we let $\mathscr{Z} = T^*M \times T^*\mathbb{R}^2 \times T^*\mathbb{R}^2$, $\mathscr{X} = C \times C_j \subset \mathscr{Z}$, and $\mathscr{Y} = T^*M \times \Delta(T^*\mathbb{R}^2) \subset \mathscr{Z}$. Note that $\mathscr{X}$ is parametrized by $x_1, x_2, \lambda, \phi, y_1, \xi_2 \in \mathbb{R}$, and we write an element of $\mathscr{Y}$ as $(s, \psi, \alpha, \beta; z_1, z_2, \eta_1, \eta_2,\ z_1, z_2, \eta_1, \eta_2)$ with all variables in $\mathbb{R}$. The intersection $\mathscr{X} \cap \mathscr{Y}$ is given by

$$\begin{aligned} &s = x_1 \cos\phi + x_2 \sin\phi, \psi = \phi, \alpha = -\lambda, \beta = \lambda(-x_1 \sin\phi + x_2 \cos\phi), \\ &x_1 = y_1 = z_1, x_2 = y_2 = z_2 = 0, -\lambda\cos\phi = 0 = \eta_1, -\lambda\sin\phi = \xi_2 = \eta_2, \end{aligned}$$

which implies that $\phi = \pm\pi/2$, so

$$\mathscr{X} \cap \mathscr{Y} = \{(0, \pm\pi/2, -\lambda, \mp\lambda x_1; x_1, 0, 0, \mp\lambda, x_1, 0, 0, \mp\lambda) : x_1, \lambda \in \mathbb{R}\}.$$

We see that the projection to T^*M is proper. Let $q \in \mathscr{X} \cap \mathscr{Y}$. To compute the tangent vector of $T_q\mathscr{X}$, we use the map $\pi : \mathbb{R}^6_{(x_1, x_2, \lambda, \phi, y_1, \xi_2)} \to \mathscr{X}$. So, a general tangent vector at q can be obtained by

$$\begin{aligned} &\pi_*(\delta x_1, \delta x_2, \delta\lambda, \delta\phi, \delta y_1, \delta\xi_2) \\ &\quad = (\delta x_2 - x_1\delta\phi, \delta\phi, -\delta\lambda, -\lambda\delta x_1 - x_1\delta\lambda, \delta x_1, \delta x_2, \lambda\delta\phi, -\delta\lambda, \delta y_1, 0, 0, \delta\xi_2). \end{aligned}$$

For the tangent vector of $T_q\mathscr{Y}$, we use the map $\rho : \mathbb{R}^8_{(s, \psi, \alpha, \beta; z_1, z_2, \eta_1, \eta_2)} \to \mathscr{Y}$ to get

$$\begin{aligned} &\rho_*(\delta s, \delta\psi, \delta\alpha, \delta\beta; \delta z_1, \delta z_2, \delta\eta_1, \delta\eta_2) \\ &\quad = (\delta s, \delta\psi, \delta\alpha, \delta\beta; \delta z_1, \delta z_2, \delta\eta_1, \delta\eta_2, \delta z_1, \delta z_2, \delta\eta_1, \delta\eta_2). \end{aligned}$$

Now we conclude that $T_q\mathscr{X} + T_q\mathscr{Y} = T_q\mathscr{Z}$ by listing 12 linearly independent tangent vectors, which is quite straightforward.

Next, consider the composition of C^* and $C_0 = T^*_qM\backslash 0$ needed in Lemma 3.4. From (8), we get

$$\begin{aligned} C^* = \{&(x_1, x_2, -\lambda\cos\phi, -\lambda\sin\phi; x_1\cos\phi + x_2\sin\phi, \phi, \\ &-\lambda, \lambda(-x_1\sin\phi + x_2\cos\phi)) : \lambda \in \mathbb{R}\backslash 0, \phi \in (-\pi, \pi), x_1, x_2 \in \mathbb{R}\}. \end{aligned} \tag{23}$$

We write

$$C_0 = \{(0, 0, \zeta_1, \zeta_2) : \zeta_1, \zeta_2 \in \mathbb{R}, \zeta_1\zeta_2 \neq 0\}.$$

Then let $\mathscr{X} = C^* \times C_0$, $\mathscr{Y} = T^*\mathbb{R}^2 \times \Delta(T^*M)$, and $\mathscr{Z} = T^*\mathbb{R}^2 \times T^*M \times T^*M$. The intersection $\mathscr{X} \cap \mathscr{Y}$ is given by

$$x_1\cos\phi + x_2\sin\phi = 0, \phi = 0, -\lambda = \zeta_1, \lambda(-x_1\sin\phi + x_2\cos\phi) = \zeta_2,$$

which implies $x_1 = 0, \phi = 0$, so

$$\mathscr{X} \cap \mathscr{Y} = \{(0, x_2, -\lambda, 0; 0, 0, -\lambda, -\lambda x_2) : \lambda, x_2 \in \mathbb{R}\}.$$

The projection to $T^*\mathbb{R}^2$ is proper. Let $q \in \mathscr{X} \cap \mathscr{Y}$. To compute the tangent vector of $T_q\mathscr{X}$, we use the map $\pi : \mathbb{R}^6_{(x_1,x_2,\lambda,\phi,\alpha,\beta)} \to \mathscr{X}$. So,

$$\begin{aligned}&\pi_*(\delta x_1, \delta x_2, \delta\lambda, \delta\phi, \delta\zeta_1, \delta\zeta_2)\\ &\quad = (\delta x_1, \delta x_2, -\delta\lambda, -\lambda\delta\phi, \delta x_1 + x_2\delta\phi, \delta\phi, -\delta\lambda, x_2\delta\lambda, \lambda\delta x_2, 0, 0, \delta\zeta_1, \delta\zeta_2).\end{aligned}$$

For the tangent vector of $T_q\mathscr{Y}$, we use $(z_1, z_2, \eta_1, \eta_2; s, \phi, \alpha, \beta; s, \phi, \alpha, \beta)$ for a general element of $\mathscr{Y}$. Consider $\rho : \mathbb{R}^8_{(z_1,z_2,\eta_1,\eta_2;s,\phi,\alpha,\beta)} \to \mathscr{Y}$, and we get

$$\begin{aligned}&\rho_*(\delta z_1, \delta z_2, \delta\eta_1, \delta\eta_2; \delta s, \delta\psi, \delta\alpha, \delta\beta)\\ &\quad = (\delta z_1, \delta z_2, \delta\eta_1, \delta\eta_2, \delta s, \delta\psi, \delta\alpha, \delta\beta, \delta s, \delta\psi, \delta\alpha, \delta\beta).\end{aligned}$$

We can also see that $T_q\mathscr{X} + T_q\mathscr{Y} = T_q\mathscr{Z}$.

Finally, we consider the composition of C^* and $\tilde{C}_j = N^*S_j\backslash 0, j = 1, 2$, needed in Lemma 3.4. In this case, we can find local coordinates (y_1, y_2) near $p \in S_j$ so that $p = 0$ and $S_j = \{y_1 = 0\}$. Thus,

$$\tilde{C}_j = \{(0, y_2, \eta_1, 0) : y_2 \in \mathbb{R}, \eta_1 \in \mathbb{R}\backslash 0\}.$$

Then let $\mathscr{X} = C^* \times \tilde{C}_j$, $\mathscr{Y} = T^*\mathbb{R}^2 \times \Delta(T^*M)$, and $\mathscr{Z} = T^*\mathbb{R}^2 \times T^*M \times T^*M$. Using (23), the intersection $\mathscr{X} \cap \mathscr{Y}$ is given by

$$x_1 \cos\phi + x_2 \sin\phi = 0, \phi = y_2, -\lambda = \eta_1, \lambda(-x_1 \sin\phi + x_2 \cos\phi) = 0,$$

which implies $x_1 = x_2 = 0$, so

$$\mathscr{X} \cap \mathscr{Y} = \{(0, 0, -\lambda\cos\phi, -\lambda\sin\phi, 0, \phi, -\lambda, 0, 0, \phi, -\lambda, 0) : \lambda, \phi \in \mathbb{R}\}$$

The projection to $T^*\mathbb{R}^2$ is proper. To compute the tangent vector of $T_q\mathscr{X}$, we use the map $\pi : \mathbb{R}^6_{(x_1,x_2,\lambda,\phi,y_2,\eta_1)} \to \mathscr{X}$. So

$$\begin{aligned}&\pi_*(\delta x_1, \delta x_2, \delta\lambda, \delta\phi, \delta\zeta_1, \delta\zeta_2)\\ &\quad = (\delta x_1, \delta x_2, -\delta\lambda\cos\phi + \lambda\sin\phi d\phi, -\delta\lambda\sin\phi - \lambda\cos\phi\delta\phi;\\ &\delta x_1\cos\phi + \delta x_2\sin\phi, \delta\phi, -\delta\lambda, -\lambda\delta x_1\sin\phi + \lambda\delta x_2\cos\phi, 0, \delta y_2, -\delta\lambda, 0).\end{aligned}$$

For the tangent vector of $T_q\mathscr{Y}$, we use $(z_1, z_2, \eta_1, \eta_2; s, \phi, \alpha, \beta; s, \phi, \alpha, \beta)$ for a general element of $\mathscr{Y}$. Let $\rho : \mathbb{R}^8_{(z_1,z_2,\eta_1,\eta_2;s,\phi,\alpha,\beta)} \to \mathscr{Y}$ to get

$$\begin{aligned}&\rho_*(\delta z_1, \delta z_2, \delta\eta_1, \delta\eta_2; \delta s, \delta\psi, \delta\alpha, \delta\beta)\\ &\quad = (\delta z_1, \delta z_2, \delta\eta_1, \delta\eta_2, \delta s, \delta\psi, \delta\alpha, \delta\beta, \delta s, \delta\psi, \delta\alpha, \delta\beta).\end{aligned}$$

Again, we can find 12 linearly independent vectors to see that $T_q\mathscr{X} + T_q\mathscr{Y} = T_q\mathscr{Z}$.

Acknowledgments. The author wishes to thank Prof. Jin Keun Seo for helpful conversations about the nonlinear nature of the beam-hardening artifacts. The author also sincerely thanks two anonymous referees for carefully reading the manuscript and making many thoughtful suggestions. In particular, the author is grateful to one of the referees for pointing out a way to simplify the proof of Lemma 4.2.

REFERENCES

[1] M. P. do Carmo, *Differential Geometry of Curves and Surfaces: Revised and Updated Second Edition*, Dover Publications, 2016.

[2] A. Greenleaf and G. Uhlmann, *Recovering singularities of a potential from singularities of scattering data*, Comm. Math. Phys., 157 (1993), pp. 549–572.

[3] V. Guillemin and G. Uhlmann, *Oscillatory integrals with singular symbols*, Duke Math. J., 48 (1981), pp. 251–267.

[4] L. Hörmander, *The Analysis of Linear Partial Differential Operators: Distribution Theory and Fourier Analysis*, 2nd ed., Springer-Verlag, 1990.

[5] L. Hörmander, *The Analysis of Linear Partial Differential Operators: Pseudo-Differential Operators*, Classics Math., Springer-Verlag, 2007.

[6] L. Hörmander, *The Analysis of Linear Partial Differential Operators* IV*: Fourier Integral Operators*, Classics Math., Springer-Verlag, 2009.

[7] A. Katsevich, *Local tomography with nonsmooth attenuation*, Trans. Amer. Math. Soc., 351 (1999), pp. 1947–1974.

[8] W. Klingenberg, *A Course in Differential Geometry*, Grad. Texts Math. 51, Springer, 2013.

[9] Y. Kurylev, M. Lassas, and G. Uhlmann, *Inverse problems for Lorentzian manifolds and non-linear hyperbolic equations*, Invent. Math., 212 (2018), pp. 781–857.

[10] F. Monard, R. Nickl, and G. Paternain, *Efficient nonparametric Bayesian inference for X-ray transforms*, Ann. Statist., 47 (2019), pp. 1113–1147.

[11] B. Palacios, G. Uhlmann, and Y. Wang, *Quantitative analysis of metal artifacts in X-ray tomography*, SIAM J. Math. Anal., 50 (2018), pp. 4914–4936, https://doi.org/10.1137/17M1160392.

[12] H. S. Park, J. K. Choi, and J. K. Seo, *Characterization of metal artifacts in X-ray computed tomography*, Comm. Pure Appl. Math., 70 (2017), pp. 2191–2217.

[13] H. S. Park, D. Hwang, and J. K. Seo, *Metal artifact reduction for polychromatic X-ray CT based on a beam-hardening corrector*, IEEE Trans. Med. Imaging, 35 (2015), pp. 480–487.

[14] H. S. Park, S. M. Lee, H. P. Kim, and J. K. Seo, *Machine-Learning-Based Nonlinear Decomposition of CT Images for Metal Artifact Reduction*, preprint, arXiv:1708.00244, 2017.

[15] A. Piriou, *Calcul symbolique non linéaire pour une onde conormale simple*, Ann. Inst. Fourier (Grenoble), 38 (1988), pp. 173–187.

[16] E. T. Quinto, *An introduction to X-ray tomography and Radon transforms*, in The Radon Transform, Inverse Problems, and Tomography, Papers from the American Mathematical Society Short Course on the Radon Transform and Applications to Inverse Problems, G. Ólafsson and E. Quinto, eds., Proc. Sympos. Appl. Math., 63, AMS Short Course Lecture Notes, American Mathematical Society, 2006, pp. 1–23.

[17] A. Sá Barreto, *Interactions of semilinear progressing waves in two or more space dimensions*, Inverse Probl. Imaging, 14 (2020), pp. 1057–1105.

[18] A. Sá Barreto and Y. Wang, *Singularities generated in the triple interaction of semilinear conormal waves*, Anal. PDE, 14 (2021), pp. 135–170.

[19] Y. Wang and Y. Zou, *Streak artifacts from non-convex metal objects in X-ray tomography*, Pure Appl. Anal., 3 (2021), pp. 295–318.

[20] Y. Zhang and H. Yu, *Convolutional neural network based metal artifact reduction in X-ray computed tomography*, IEEE Trans. Med. Imaging, 37 (2018), pp. 1370–1381.